



## A Methodology to Estimate the Signal-to-Interference Power Ratio for Intermittent Disturbances

Artur N. de São José<sup>(1)</sup>, Eric Pierre Simon<sup>(1)</sup>, Alexandre Boé<sup>(1)</sup>, Thomas Vantrois<sup>(1)</sup>, Christophe Gransart<sup>(2)</sup>  
and Virginie Deniau<sup>\*(2)</sup>

(1) Univ. Lille, CNRS, USR 3380 - IRCICA - Institut de Recherche sur les Composants logiciels et matériels pour l'Information et la Communication Avancée, F-59000 Lille, France

(2) COSYS-LEOST, Univ Gustave Eiffel, IFSTTAR, Univ Lille, F-59650 Villeneuve d'Ascq, France

### Abstract

Estimating the signal-to-interference power ratio with traditional measuring equipment such as spectrum analyzers is not an easy task when the disturbance is intermittent. In these situations, the power may rapidly switch between its peak value and the equipment noise floor. As a consequence, instantaneous values obtained with a marker do not faithfully represent the actual signal power. In this paper, we propose a methodology to overcome such an issue, based on the post-processing of oscilloscope measurements. Although we use it to estimate critical signal-to-interference power ratios of a LoRa system, it can be used to calculate any power ratio.

### 1 Introduction

Electromagnetic compatibility (EMC) researchers are increasingly concerned with non-standard electromagnetic interference (EMI). The immunity of devices and systems against the most common disturbances is already evaluated in a traditional EMC validation process. The radiated immunity test standard ISO 11452-2 [1], for example, does not take into account intermittent EMI, *i.e.* those that constantly enter and leave the receiver frequency band. Given the complex behavior of some non-standard signals (see *e.g.* the transient disturbances described in [2]), it is usually difficult to predict their effects. Consequently, the immunity of electrical devices and systems to such disturbances, which can be either intentional or non-intentional, is not usually assessed in the design phase. In this work, we are mainly concerned with the impact of intentional EMI (IEMI) over long range (LoRa)-based railway communication systems. However, the methodology that we present here is extensive to non-intentional EMI, as well as to other communication systems.

### 2 LoRa technology and interference model

LoRa defines the physical layer protocol and LoRaWAN is an open standard defining the medium access control (MAC) protocol. LoRaWAN has three different classes of end-point devices to address the different needs, namely Class A, B and C. Class A has the lowest costs and energy

consumption rates and is mainly used for internet of things. Class A nodes initiate the communication with the gateway through a pure ALOHA medium access. The transmission is followed by two short downlink windows to receive a response from the gateway. The response consists of an acknowledgement (ACK). If the ACK is received in the first window, the second one is disabled [3]. In our investigations, we use the presence of the ACK as an indicator of a correct transmission

In LoRa, each symbol has SF bits ( $7 \leq SF \leq 12$ ), where SF stands for spreading factor. It represents  $M = 2^{SF}$  possible values. The signal bandwidth is denoted by  $B$ , and the symbol duration is  $T_s = MT$ , where  $T = 1/B$ . Each symbol, also called chirp, is a linear frequency shift over  $T_s$ . It is built from a raw chirp  $c(t)$  with an instantaneous frequency  $\frac{B}{T_s}t$ , yielding to the following base-band expression [3]:

$$c(t) = \exp\left(j2\pi\frac{B}{2T_s}t^2\right) \quad t \in \left[-\frac{T_s}{2}, \frac{T_s}{2}\right]. \quad (1)$$

The LoRa symbol is obtained by performing a cyclic shift of the raw chirp by  $mT$ , where  $m \in \{0, \dots, M-1\}$  is the data to be transmitted. The jamming signals studied here are also raw chirps but with considerably smaller periods, as classically found in jammers – see Fig. 1. For this reason, it is only necessary to adapt Eq. 1 to obtain a mathematical model for a typical periodic frequency-modulated jamming signal [4]. To do so, one must replace  $T_s$  by  $T_{jam}$ , the jamming sweep time and  $B$  by the jamming bandwidth,  $B_{jam}$ . Nevertheless, since these are not the only spurious signals present in the railway environment, solid techniques become necessary to estimate the signal-to-noise and signal-to-interference power ratios (SNR and SIR) in order to evaluate the LoRa communication integrity.

### 3 The test bench

#### 3.1 General description

In order to analyze the interaction between the LoRa signal and the jamming one, we use the test bench setup shown in Fig. 2. It is used to generate LoRa signals and to combine

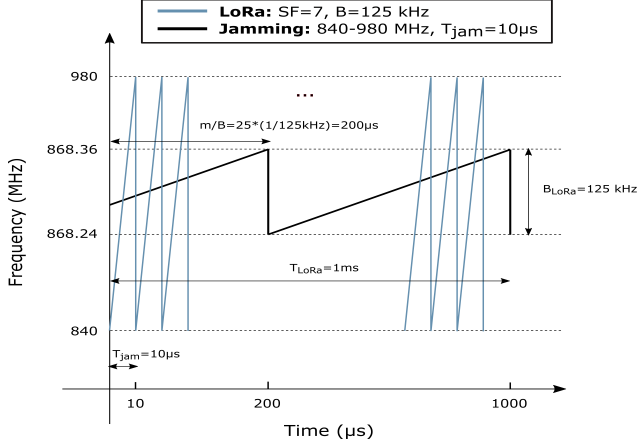


**Figure 1.** Out-of-scale spectrograms. LoRa (black) and jamming (blue) signals with typical parameters.

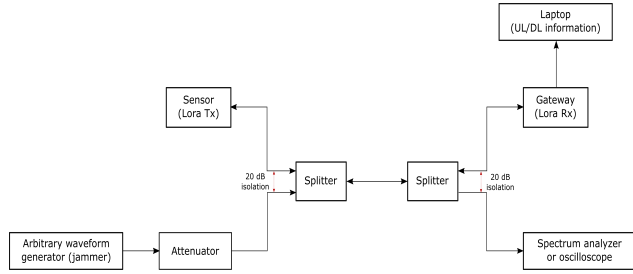


**Figure 2.** Architecture of the test bench.

them with spurious jamming waveforms. The useful signals are obtained with a generic LoRa device. Four LoRa configurations<sup>1</sup> are under investigation. ChirpStack, an open-source software, is used here to set the LoRa parameters and monitor the uplink (UL) and downlink (DL) data (ACK). Additionally, 16 jamming signal configurations are set with an arbitrary waveform generator<sup>2</sup>. The LoRa central frequency is set to 868.3 MHz and the bandwidth to 125 kHz, while the jamming signal occupies the 840 - 980 MHz band. To control the SIR, we dynamically change the settings of the attenuator, which is connected to the waveform generator output. Finally, we evaluate the signals using two measuring equipment: an oscilloscope and a spectrum analyzer. An important remark is that we use cables (instead of antennas) to connect the devices. By doing so, we avoid that other phenomena – such as EMI from other signals or antenna misalignment – affect the measurements.

### 3.2 Spectrum analyzer limitations

The jamming signal dynamic imposes difficulties to the power measurement process – and therefore to the SIR calculation. Since it is much faster and has a much wider bandwidth compared to the LoRa signal, it will constantly enter and leave the communication channel. This behavior is in turn influenced by the particular sweep time chosen.

<sup>1</sup>(SF,CR)=(7,4/5),(7,4/8),(12,4/5),(12,4/8). CR stands for Code Rate.

<sup>2</sup>Sweep period ( $\mu$ s): 1-10,15,20,30,40,50,100.

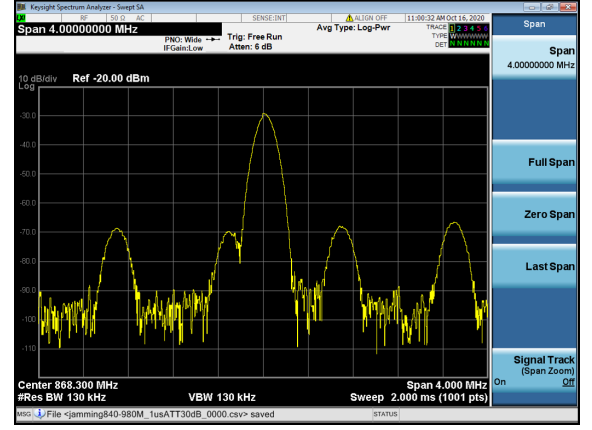


**Figure 3.** Spectrum analyzer measurement (LoRa and jamming signal,  $T_{jam} = 1 \mu$ s).

To better explain how these characteristics can affect the power measurements, we show in Fig. 3 a spectrum analyzer screenshot. The central peak corresponds to the LoRa signal and the other four peaks come from the jamming signal spectrum in the 866.3 - 870.3 MHz range. The spacing between the jamming signal spectral components is 1 MHz, which corresponds to the inverse of its sweep period ( $1 \mu$ s in this case). As a result of this particular energy distribution, one of these four components is only partially present in the LoRa channel. Therefore, if we use a marker located in one of these four peak values, it will not contain the actual jamming power seen by a LoRa receiver.

The solution in this case is to use a configuration called '0 Hz span'. In this mode, the spectrum analyzer no longer performs the frequency sweep. Instead, it only reads the power seen by an user-defined band-pass filter, rejecting thus the out-of-band energy. Since we want to read the same power seen by the LoRa gateway, we set the spectrum analyzer central frequency to 868.3 MHz and its resolution bandwidth (RBW) to 130 kHz (it was not possible to adjust the RBW to the actual LoRa channel bandwidth, *i.e.* 125 kHz). The result can be seen in Fig. 4 for two different sweep times:  $4 \mu$ s and  $30 \mu$ s. Figure 4 contains power *versus* time plots. Each of them essentially contains UL, ACK and jamming signals. Thanks to the -30 dB attenuator placed between the LoRa transmitter and the first splitter, it is possible to distinguish between the UL and ACK signals. Figure 4 reveals that these two signals have a relatively stable behavior in time domain, differing in terms of power level and duration. Therefore, it is reasonable to use a marker to obtain the corresponding peak power levels (for SIR calculations, the ACK power level is not used). However, the jamming signal (highlighted with circles and dashed lines in Fig. 4) is extremely unstable and the instability apparently increases with the sweep time. In this scenario, the peak value is no longer a good metric and thus we cannot proceed with the analyses in these cases. In the following sections, we describe a methodology to overcome this problem using an oscilloscope and a compu-

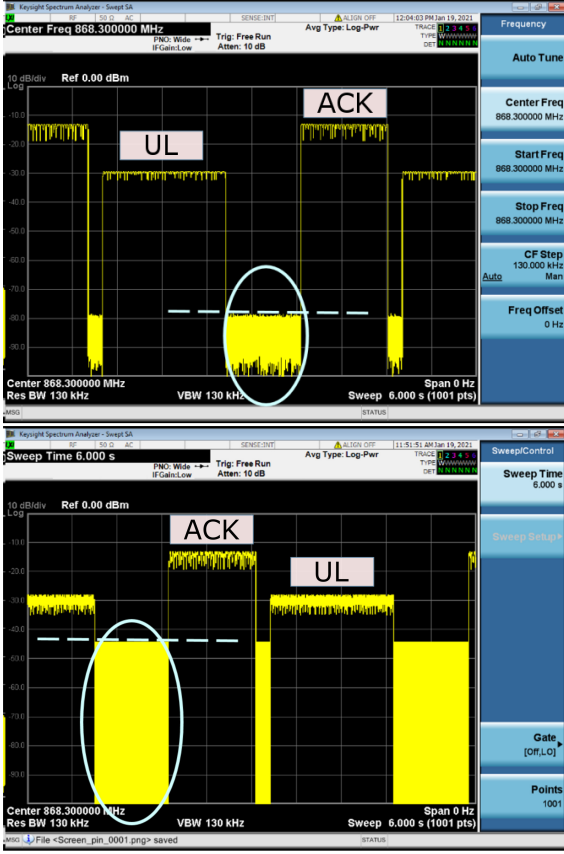


**Figure 4.** Spectrum analyzer measurements (0 Hz span); top: sweep time = 4  $\mu$ s, bottom: sweep time = 30  $\mu$ s.

tational routine.

## 4 Methodology

Our methodology is divided in two parts. In a first moment, we try to identify critical conditions which result in communication breakdown. After that, we effectively estimate the LoRa and jamming signal power levels, which allows us to calculate the SIR. Both stages are based on the test setup shown in Fig. 2. Figure 5 contains a flowchart that summarizes the first stage of our methodology. The first two steps consists in turning on both the LoRa and jamming signal sources. After that, we set the attenuation level to 50 dB. Although not useful to precisely measure the signal power, the spectrum analyzer can be used to detect the communication breakdown. For this reason, we activate the '0 Hz span' mode, and observe how the UL and ACK signals evolve with time. If the ACK signal is corrupted or absent, we consider that the link between the sensor and gateway is lost, and we have reached the critical SIR. In this case, we register the corresponding attenuation level. If this is not verified, we reduce the attenuation and continue the process until a loss of communication occurs or until the attenuation is equal to 0 dB.

In the second stage, we continue to use the test setup from Fig. 2. However, we do not simultaneously activate the

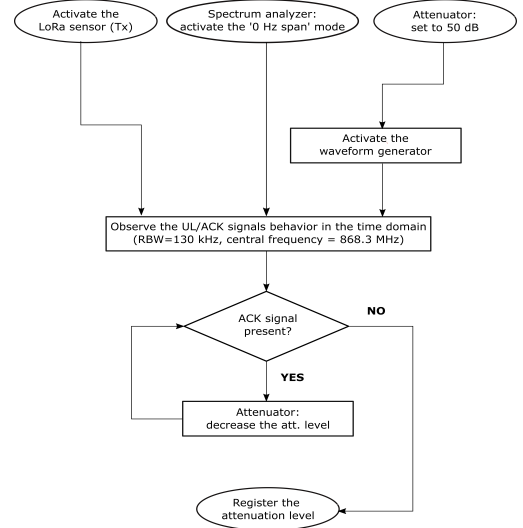


**Figure 5.** Process to identify critical attenuation levels.

LoRa and jamming signal sources. Instead, we analyze one signal at a time. The analysis is performed using an oscilloscope set with 10 GSa/s. The attenuator is set to 0 dB and we do not change this value during the experiments. The sampling frequency of the oscilloscope was set to 10 GSa/s and the signals were acquired during a 1 ms long time window. This is exactly the length of one LoRa chirp (*i.e.* one symbol),  $T_s = 2^{SF} / B$  ( $B$  is the bandwidth), when the SF is equal to 7. However, this is approximately 3% of a LoRa symbol time when SF=12 (we used both SF=7 and SF=12). We did that to avoid creating large files, which are of difficult storage and processing. However, since both LoRa and jamming signal waveforms have constant amplitude, we believe the window length does not significantly affect the power calculations.

Once these two signals are acquired, we process them using MATLAB. Since we are interested in the total power that would be seen by a LoRa receiver, we need to implement a band-pass filter (or a low-pass filter if the signal is down-converted to the base-band) with a bandwidth equal to 125 kHz. To do so, we implemented a Gaussian filter in MATLAB by Fourier transforming an impulse response obtained with the *gausswin* command. To use this function, we set  $\alpha = 250$ , where  $\alpha = (L - 1) / (2\sigma)$ ,  $L$  is the filter length, and  $\sigma$  is the standard deviation of the Gaussian function. Ideally, we should use the same type of filter present in LoRa receivers. Nevertheless, to the best of our knowledge, this information is not publicly available. So, we chose the same filter used by the spectrum analyzer. Once the signals are filtered, we calculate the respective average power levels. Finally, we calculate the SIR by dividing the LoRa power by the jamming signal power, and taking the logarithm of the resulting value. The second stage of our methodology can be summarized as follows.

- **Step 1:** set the attenuation to 0 dB and activate the waveform generator.

- **Step 2:** export the jamming signal waveform from the oscilloscope to an USB flash drive.
- **Step 3:** turn off the waveform generator and activate the LoRa transmitter.
- **Step 4:** export the LoRa signal waveform from the oscilloscope to an USB flash drive.
- **Step 5:** import the signals in a computer and apply a 125 kHz bandwidth filter.
- **Step 6:** calculate the average powers and use them to calculate the non-critical SIR.
- **Step 7:** add the attenuation levels found in the first step of the methodology to the values obtained in Step 6 in order to obtain the critical SIR.

## 5 Results

The main results refer to the critical SIR calculation using the proposed methodology. In order to establish a benchmark analysis, we additionally evaluated it using two other techniques. The first one is based on a visual inspection of the spectrum analyzer results in the '0 Hz span' mode – this method contains limitations, as discussed in Section 3.2. The second alternate method is based on analytical models based on Eq. 1, serving thus as a reference.

Figure 6 shows the results in terms of critical SIR *versus* sweep time graphs in two different scales. The three approaches provide the same qualitative behavior: a quick decay, which stabilizes when the sweep time is approximately 5  $\mu s$ . This result suggests that the simulated LoRa system is more susceptible to very fast jammers. This figure also evidences the differences between the three estimates. Although it can reach up to 6 dB for long sweep times, the major difference occurs when  $T_{jam} = 1 \mu s$ . This can be explained as follows. The spectral components of the jamming signal are almost out of the LoRa channel for this particular sweep time value, as seen in Fig. 3. Therefore, the only thing that the filter will measure is the equipment noise floor. During our measurements, we observed that the spectrum analyzer and oscilloscope noise floor levels are approximately -100 dBm and -120 dBm. This explains the fact that the SIR oscilloscope estimate is approximately 20 dB above that obtained with the spectrum analyzer. The analytical model, on the other hand, is only subject to hardware limitations. Therefore, the corresponding noise floor is much lower in this case, which explains the very high SIR estimate. Finally, we highlight that the best global performance was obtained with the oscilloscope: it presents 84.96 % of correlation with the reference curve, against 66.79 % obtained between spectrum analyzer and model.

## 6 Conclusions

In this work, we proposed and evaluated a method to calculate the SIR of communication systems under intermit-

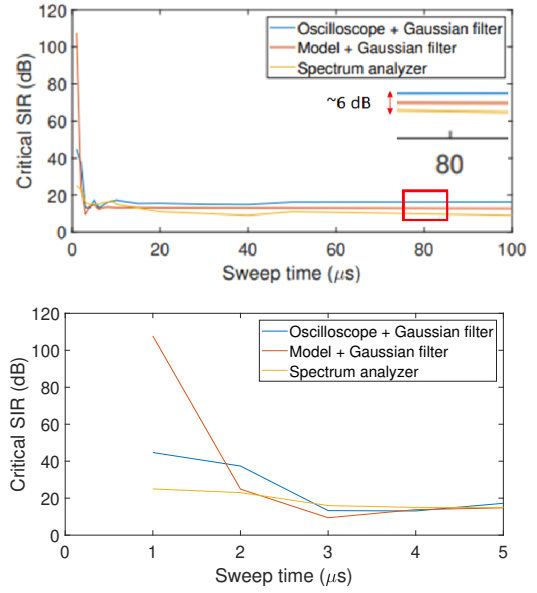


**Figure 6.** SIR estimates as functions of the sweep time.

tent EMI. The obtained results have more correlation with the mathematical models than those obtained with the spectrum analyzer. Concerning our specific case study, results suggests that the simulated LoRa system can be more susceptible to jamming chirps with a duration less than 5  $\mu s$ .

## 7 Acknowledgements

This work was performed in the framework of the LoRa-R project, which is co-financed by the European Union with the European Regional Development Fund, the Hauts de France Region Council, and the SNCF railway company.

## References

- [1] V. Rodriguez. Automotive component emc testing: Cspr 25, iso 11452-2 and equivalent standards. *IEEE Electromagnetic Compatibility Magazine*, 1(1):83–90, 2012.
- [2] M. Maarleveld, K. Kreisch, H. Kellerbauer, and K. Friedrich. Investigation on the propagation of disturbing pulses in traction batteries of electric and hybrid vehicles. In *2014 International Symposium on Electromagnetic Compatibility*, pages 391–395, 2014.
- [3] A. A. Tesfay, E. P. Simon, I. Nevat, and L. Clavier. Multiuser detection for downlink communication in lora-like networks. *IEEE Access*, 8:199001–199015, 2020.
- [4] V. Deniau, C. Gransart, G. L. Romero, E. P. Simon, and J. Farah. Ieee 802.11n communications in the presence of frequency-sweeping interference signals. *IEEE Transactions on Electromagnetic Compatibility*, 59(5):1625–1633, 2017.